PAPER

Check for updates

Dielectric response of light, heavy and heavy-oxygen water: isotope effects on the hydrogen-bonding network's collective relaxation dynamics†

Bence Kutus, [iD] [a] Andrey Shalit,[b] Peter Hamm[b] and Johannes Hunger [iD] *[a]

Isotopic substitutions largely affect the dielectric relaxation dynamics of hydrogen-bonded liquid water; yet, the role of the altered molecular masses and nuclear quantum effects has not been fully established. To disentangle these two effects we study the dielectric relaxation of light ($H_2^{16}O$), heavy ($D_2^{16}O$) and heavy-oxygen ($H_2^{18}O$) water at temperatures ranging from 278 to 338 K. Upon $^{16}O/^{18}O$ exchange, we find that the relaxation time of the collective orientational relaxation mode of water increases by 4–5%, in quantitative agreement with the enhancement of viscosity. Despite the rotational character of dielectric relaxation, the increase is consistent with a translational mass factor. For H/D substitution, the slow-down of the relaxation time is more pronounced and also shows a strong temperature dependence. In addition to the classical mass factor, the enhancement of the relaxation time for $D_2^{16}O$ can be described by an apparent temperature shift of 7.2 K relative to $H_2^{16}O$, which is higher than the 6.5 K shift reported for viscosity. As this shift accounts for altered zero-point energies, the comparison suggests that the underlying thermally populated states relevant to the activation of viscous flow and dielectric relaxation differ.

Introduction

The substitution of hydrogen for deuterium in water has strong impact on its dynamic properties, such as viscosity,[1–5] translational and rotational self-diffusion,[5,6] resonance frequency of molecular vibrations,[5,7] echo decay time for hydrogen-bond vibrations obtained from Raman-terahertz (THz) spectroscopy,[8] as well as dipole–dipole correlation times measured by dielectric relaxation[9–15] and THz time-domain spectroscopies.[16–18] Relative to light water ($H_2^{16}O$), the different dynamics of heavy water ($D_2^{16}O$) can be largely explained by the altered strength of its hydrogen-bonding network, which arises from nuclear quantum effects,[5,8,19–25] *e.g.* different zero-point energy and reduced delocalization of deuterium due to its higher nuclear mass.[5] Despite these differences, numerous dynamic properties of $H_2^{16}O$ and $D_2^{16}O$ collapse onto a single curve when nuclear quantum effects are accounted for by an apparent temperature shift, ΔT.[2–4,8,16] That is, the properties of $D_2^{16}O$ at $T + \Delta T$ equal those of $H_2^{16}O$ at T, reflecting that increased thermal fluctuations of $D_2^{16}O$ mimic enhanced quantum fluctuations of $H_2^{16}O$.[8,19,20,23,26,27]

Besides these nuclear quantum effects, classical mechanics already predict a change in the properties of water for different isotopes due to their different nuclear masses.[5] To assess these classical mass effects, it is instructive to compare the properties of $H_2^{16}O$ to those of $D_2^{16}O$ and heavy-oxygen water, $H_2^{18}O$.[1,5,8,28,29] Both, $^{16}O/^{18}O$ and H/D substitutions, result in a nearly identical increase in the molecular mass of water. For instance, these increased masses give rise to a trivial increase in the volumetric densities.[28] For molecular vibrations, for which resonance frequencies scale with the inverse square root of the oscillators' reduced mass, isotope shifts due to classical mass effects are most pronounced for H/D exchange: the center frequency of the OD stretching band is $\sim \sqrt{2}$ times lower than the OH stretching frequency, whereas heavy oxygen – which increases the reduced mass only by $\sim 0.6\%$ – hardly affects these local dynamics.[5,7]

In case of collective dynamics involving more than one water molecule, classical mass effects are arguably less straightforward to predict. The macroscopic viscosity is one example for properties that reflect such non-local dynamics.[30–33] For non-associated liquids, Eyring proposed as early as in 1936 that the thermally activated translation of a single molecule provides a good description for viscous flow, which in turn predicts viscosity to scale with the square root of the molecular mass.[34] For hydrogen-bonded liquids, however, correlated molecular motions, *i.e.* the restructuring of the hydrogen-bonding network alters viscosity.[30–33]

[a] *Department of Molecular Spectroscopy, Max Planck Institute for Polymer Research, Ackermannweg 10, 55128 Mainz, Germany. E-mail: hunger@mpip-mainz.mpg.de*
[b] *Department of Chemistry, University of Zurich, Winterthurerstrasse 190, 8057 Zurich, Switzerland.*
† Electronic supplementary information (ESI) available. See DOI: 10.1039/d0cp06460b

This journal is © the Owner Societies 2021

Phys. Chem. Chem. Phys., 2021, **23**, 5467–5473 | **5467**

This structural rearrangement also involves rotational motions of water molecules,[33,35,36] for which the rate scales with the inverse square root of the moments of inertia.[6] Viscometric experiments using isotopic $^{16}O/^{18}O$ substitution, which alters the moments of inertia of a water molecule by $\sim0.6\%$ but increases its molecular mass by $\sim13\%$, have however shown that the $\sim5\%$ increase in viscosity is consistent with a translational mass factor, $\sqrt{M(H_2{}^{18}O)/M(H_2{}^{16}O)}$.[1] Conversely, the substantial increase in viscosity (15–30%) upon H/D exchange is largely attributed to nuclear quantum effects.[2,8] Empirically, this enhancement has been modelled using the same translational mass factor (5%) as found for $^{16}O/^{18}O$ substitution and an apparent temperature shift of 6.5 K to account for (temperature-dependent) nuclear quantum effects.[2–4,8] Yet, for translational diffusion – which is intimately related to viscosity – the ratio of diffusivities of $H_2{}^{16}O$ and $D_2{}^{16}O$ seems to be even lower than the translational mass factor at elevated temperatures.[5] Based on MD simulations,[36] such deviations have been attributed to coupling to rotational motions. Furthermore, Raman-THz echoes have been shown to be rather insensitive to classical mass effects,[8] despite their correlation with structural aspects related to viscosity of aqueous solutions.[37] As such, the role of isotope effects in the collective dynamics of water has remained elusive.

Such collective dynamics are also reflected in the dynamics probed with dielectric relaxation spectroscopy (DRS), which is sensitive to dipolar reorientation of an ensemble of water molecules. At 298 K, the dielectric spectrum of water is dominated by an intense relaxation mode centered at ~20 GHz, which is attributed to dipole fluctuations upon rearrangement of the hydrogen-bonding network.[38–42] To quantitatively reproduce the static permittivity of water using *ab initio* molecular dynamics simulations, correlated motion of water molecules across a few hydration shells has to be taken into account, which has led to the notion that dielectric relaxation reports on the collective relaxation dynamics of water.[43] Despite the collectivity of the detected dynamics, the corresponding relaxation time of 8.3 ps at 298 K is consistent with what one would expect for uncorrelated, diffusive motion of dipolar water molecules in the liquid phase and the variation of the relaxation time with temperature is correctly predicted by the Stokes–Einstein–Debye equation over a remarkably wide temperature range.[44–46] Hence, viscous friction appears to dominate the dielectric relaxation dynamics. Consistent with this notion, the relaxation time of water increases upon H/D exchange.[9–16] Yet, the increase in viscosity and the increase in relaxation time upon H/D exchange do not agree quantitatively[6,9] and are certainly different for $H_2{}^{16}O/D_2{}^{16}O$ mixtures.[12] Therefore, in addition to altered viscosity, librational and vibrational motions have been invoked to explain the slow-down of the dipolar reorientation dynamics.[12] Overall, besides water in the gas-phase, where the variation of rotational transitions are accurately predicted by the altered moments of inertia,[47] the origin of isotope effects in dielectric relaxation dynamics is not yet fully understood. In particular, the role of classical mass and nuclear quantum effects has not been disentangled.

In this work, we separate such classical mass effects from nuclear quantum effects by studying the broadband dielectric response of $H_2{}^{16}O$, $H_2{}^{18}O$, and $D_2{}^{16}O$ at temperatures ranging from 278 to 338 K to provide a unifying view on isotope effects on the dielectric response of water. In line with previous findings, we observe that, relative to $H_2{}^{16}O$, $D_2{}^{16}O$ exhibits a significantly reduced orientational relaxation rate, whereas the relaxation of $H_2{}^{18}O$ slows down to a lesser extent. We find that the corresponding increase in the relaxation time and the increase in viscosity are strongly correlated for both $D_2{}^{16}O$ and $H_2{}^{18}O$. The longer relaxation time of $H_2{}^{18}O$ can be fully accounted for by the increased viscosity, suggesting that the isotope enhancement for both observables are determined by the same classical mass effect. On the other hand, nuclear quantum effects upon H/D substitution result in a temperature dependent retardation of the relaxation dynamics of $D_2{}^{16}O$ (as compared to $H_2{}^{16}O$) and the relative enhancement of the relaxation time slightly exceeds the relative increase in the viscosity.

Experimental

Materials

For dielectric measurements, de-ionized $H_2{}^{16}O$ was obtained from a Milli-Q purification system (18.2 MΩ cm, Merck Millipore). $D_2{}^{16}O$ (99.90 atom% D, Eurisotop) and $H_2{}^{18}O$ (97 atom% ^{18}O, Sigma-Aldrich) were used as received. Prior to each measurement, fresh aliquots of $H_2{}^{16}O$ were obtained. $D_2{}^{16}O$ and $H_2{}^{18}O$ were stored in tight-lid glass vials.

Dielectric relaxation spectroscopic measurements (DRS)

DRS probes the frequency-dependent macroscopic polarization of a sample induced by a low-amplitude, oscillating electric field with field frequency ν,[48] commonly expressed in terms of the complex permittivity, $\varepsilon'(\nu)$:

$$\hat{\varepsilon}(\nu) = \varepsilon'(\nu) - i\varepsilon''(\nu) \tag{1}$$

where $\varepsilon'(\nu)$ and $\varepsilon''(\nu)$ are the frequency-dependent dielectric permittivity and loss representing the real and imaginary components of polarization, respectively. For dipolar liquids, polarization at microwave frequencies predominantly stems from rotational motion of species with a permanent dipole moment. Upon applying an external field with low frequency, a molecular ensemble will rearrange according to the field resulting in a polarization as measured by ε'. With increasing field frequency, molecules cannot instantaneously follow the oscillating field, giving rise to a decrease in ε' and a peak in ε''.

In the present study, $\hat{\varepsilon}(\nu)$ spectra were recorded using an Anritsu Vector Network Analyzer (model MS4647A). The range $0.05 \leq \nu/\text{GHz} \leq 50$ was covered using a frequency-domain reflectometer, equipped with a coaxial open-ended probe based on 1.85 mm connectors. Measurements at $50 \leq \nu/\text{GHz} \leq 125$ were performed using an open-ended probe, connected with 1 mm connectors to an external frequency converter module (Anritsu 3744A mmW).[15] To calibrate the setup, air, conductive

5468 | *Phys. Chem. Chem. Phys.*, 2021, **23**, 5467–5473

This journal is © the Owner Societies 2021

silver paint, and H$_2^{16}$O were used as calibration standards using the dielectric spectra of H$_2^{16}$O reported in literature.[15]

The temperature was varied from 278 to 338 K at increments of 10 K. To maintain constant temperature, the samples were placed into a double-walled sample holder connected to a Julabo F12-ED thermostat. The temperature stability in the center of the sample was estimated to be ±0.5 K. The spectra were recorded 6–8 times for each water isotope and this set of experiments was repeated at least once.

Results and discussion

Spectral analysis and qualitative trends

In Fig. 1a we show the dielectric spectrum of H$_2^{18}$O at 298 K, which exhibits a dominant relaxation at ∼20 GHz. This relaxation is characterized by a dispersion in ε' and a peak in ε''. For H$_2^{16}$O, this relaxation mode has been attributed to the collective rearrangement of its three-dimensional hydrogen-bonding network[38–42] and can be excellently described by a Debye-type relaxation with its center position characterized by the collective relaxation time, τ_c. At higher frequencies (>50 GHz), the spectra of water deviate from a single Debye relaxation,[13,15–17,39–41,45,49–53] which is often accounted for by an additional Debye relaxation – the so-called fast relaxation – with relaxation time τ_f.[13,15–17,39,45,49,50,53] In line with these earlier studies, we model the experimental spectra of all three isotopic species of water with a combination of two Debye-type relaxations:

$$\hat{\varepsilon}(\nu) = \frac{S_c}{1 + i2\pi\nu\tau_c} + \frac{S_f}{1 + i2\pi\nu\tau_f} + \varepsilon_\infty - \frac{i\kappa}{2\pi\nu\varepsilon_0} \quad (2)$$

where S_c and S_f are the relaxation strengths (amplitudes) of the collective and the fast Debye relaxation, respectively. ε_∞ is the infinite-frequency permittivity, which comprises polarization contributions at frequencies above our experimentally accessible range. The corresponding static dielectric constant, ε_s, equals to $S_c + S_f + \varepsilon_\infty$. The last term of eqn (2) accounts for (minor) contributions due to the dc conductivity, κ, of the samples. ε_0 is the permittivity of free space. We note that the thus obtained conductivities ($\kappa < 0.01$ S m^{-1}) reflect the experimental uncertainty (given by the accuracy of the calibration with conductive silver paint), rather than the sample conductivity.

To reduce the parameter space when fitting eqn (2) to the data, we constrain ε_∞ for H$_2^{16}$O and H$_2^{18}$O to the values reported for H$_2^{16}$O in ref. 15 (based on the similarity of their other physical properties[1,28,29]) and for D$_2^{16}$O to the values reported in the same reference. We perform the fits for each spectrum individually by minimizing the sum of the squared deviations between simulated and experimental data on a logarithmic scale. For all three water isotopes, the averages of the thus obtained parameters and the corresponding error bars (estimated as three times the standard deviation) are listed in Tables S1–S3 in the ESI.†

Similar to previous findings for H$_2^{16}$O[13,15–17,39,45,49,50,53] (see also Fig. S1a, ESI†), we find that eqn (2) provides an excellent fit for the experimental $\hat{\varepsilon}(\nu)$ spectra for H$_2^{18}$O (Fig. 1a) and D$_2^{16}$O (Fig. S1b, ESI†). The experimental frequency range of this work fully covers the collective relaxation, reflected by low relative errors of the corresponding relaxation parameters for ε_s, S_c and τ_c (Tables S1–S3, ESI†). For S_f and τ_f, the experimental uncertainties are higher, since the center of the fast relaxation (H$_2^{16}$O: ∼650 GHz, D$_2^{16}$O: ∼550 GHz at 298 K[15,17]) is beyond the detected frequency range, in particular at elevated temperatures. Thus, we restrict the quantitative analysis to the collective relaxation.

In Fig. 1b, the fitted dielectric losses for all studied isotopic species at four temperatures are displayed. For each species, we observe a shift of the dominant relaxation to higher frequencies upon increasing temperature, which demonstrates that the relaxation is thermally activated. Simultaneously, the relaxation strength (i.e. $S_c + S_f$, the area of the loss peaks; see Fig. S2, ESI†) markedly decreases, as enhanced thermal fluctuations counter dipolar alignment.[54,55]

Upon isotopic substitution, we find the loss peak for D$_2^{16}$O to shift to lower frequencies at all temperatures as compared to H$_2^{16}$O, consistent with previous studies.[9–15] This red-shift is also reflected by the longer τ_c relaxation times of D$_2^{16}$O (Fig. 2). For H$_2^{18}$O, we detect a weaker, yet significant, shift to lower frequencies, which is again accompanied by the higher values of τ_c (Fig. 2). As such, we find that not only H/D exchange, but also ^{16}O/^{18}O substitution slows down the (dipolar) rotational relaxation of water. For the relaxation time of the fast mode, τ_f (inset in Fig. 2), the scatter of the data does not allow to discern a clear trend, as the values are the same within experimental error for the three species below 308 K. The increase in τ_f(D$_2^{16}$O) above 308 K parallels the decrease in S_f(D$_2^{16}$O), indicative of strong correlation of these two fitted parameters (see the inset in Fig. S2, ESI†). As such, the higher values of τ_f(D$_2^{16}$O), relative to τ_f(H$_2^{18}$O) and τ_f(H$_2^{16}$O), above 308 K
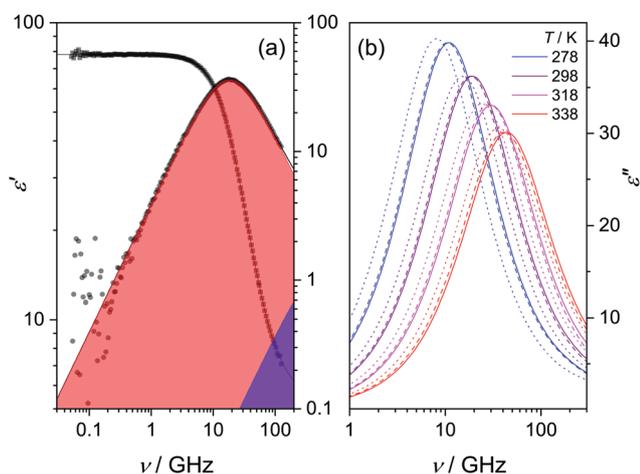
Fig. 1 (a) Relative permittivity (ε', left axis) and dielectric loss (ε'', right axis) spectra of H$_2^{18}$O at 298 K. Squares and circles represent the experimental ε' and ε'' data, respectively; the black solid lines show the fits using eqn (2). Red and purple shaded areas depict the contribution of the cooperative and fast relaxation modes to ε'', as obtained from the fit. For visual clarity, the last term of eqn (2) was subtracted from ε''. (b) Comparison of the ε'' spectra of H$_2^{16}$O (solid lines), H$_2^{18}$O (dashed lines) and D$_2^{16}$O (dotted lines), respectively, at selected temperatures as obtained from the fits using eqn (2).

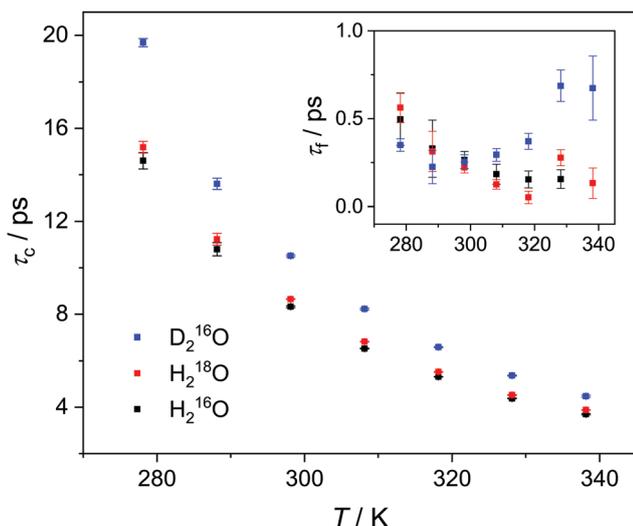This journal is © the Owner Societies 2021

Phys. Chem. Chem. Phys., 2021, **23**, 5467–5473 | **5469**

Fig. 2 Relaxation time of the collective relaxation (τ_c) for $H_2^{16}O$, $H_2^{18}O$ as well as $D_2^{16}O$ as a function of temperature, as obtained by fitting eqn (2) to the experimental complex permittivity spectra. Inset: Relaxation time of the fast relaxation (τ_f). The corresponding error bars represent the triple standard deviation.

presumably reflect the shift of the fast relaxation to frequencies significantly higher than those covered by our experiments.

The effect of temperature on the relaxation time of the cooperative mode

To quantify the thermal activation of τ_c, we use the Eyring theory,[39,56] which assumes that the relaxation pathway passes through a thermally activated transition state:

$$\ln\frac{\tau_c k_B T}{h} = \frac{1}{RT}\left(\Delta H^{\#} - T\Delta S^{\#}\right) \quad (3)$$
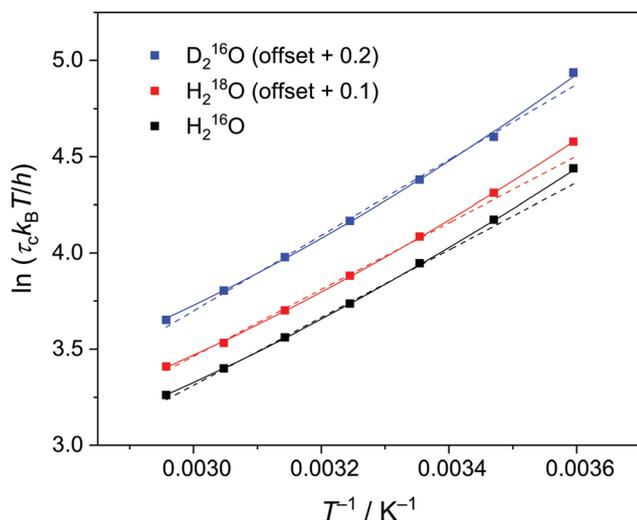

Fig. 3 Eyring plot for the relaxation time of the collective relaxation (τ_c) for $H_2^{16}O$, $H_2^{18}O$, and $D_2^{16}O$. Symbols represent the experimental data, while dashed and solid lines are the results of the fits using eqn (3) and (3)–(5), respectively. The corresponding error bars are smaller than the size of the symbols. For visual clarity, the data of $H_2^{18}O$ and $D_2^{16}O$ are offset by 0.1 and 0.2, respectively, along the vertical axis.

where $\Delta H^{\#}$ is the enthalpy, and $\Delta S^{\#}$ is the entropy of activation. k_B, h, and R are the Boltzmann, Planck, and gas constants, respectively, and T is the thermodynamic temperature. Using this approach, we find that assuming $\Delta H^{\#}$ and $\Delta S^{\#}$ to be independent of temperature does not fully reproduce the observed variation of τ_c as a function of temperature: the experimental $\ln\frac{\tau_c k_B T}{h}$ values *versus* $1/T$ deviate from linearity (see eqn (3), dashed lines in Fig. 3), in agreement with previous findings.[39,42,45,57] This deviation indicates that $\Delta H^{\#}$ and $\Delta S^{\#}$ are temperature-dependent, which can be accounted for by the isobaric heat capacity of activation, $\Delta c_p^{\#}$:[39,57]

$$\Delta H^{\#} = \Delta H_{ref}^{\#} + \Delta c_p^{\#}\left(T - T_{ref}\right) \quad (4)$$

$$\Delta S^{\#} = \Delta S_{ref}^{\#} + \Delta c_p^{\#}\ln\frac{T}{T_{ref}} \quad (5)$$

where $\Delta H_{ref}^{\#}$ and $\Delta S_{ref}^{\#}$ are the activation parameters at T_{ref}, which we set to 298 K. As demonstrated in Fig. 3, using $\Delta c_p^{\#}$ to account for temperature dependent activation parameters captures the slight curvature of the Eyring plot very well. The extracted values of $\Delta H_{ref}^{\#}$ and $\Delta S_{ref}^{\#}$ (Table 1) are in line with previous literature results for $H_2^{16}O$ and $D_2^{16}O$, while the values for $\Delta c_p^{\#}$ are somewhat lower than those reported earlier.[39,57]

Comparison of the activation parameters shows that thermal activation for the dipolar relaxation of $H_2^{18}O$ and $H_2^{16}O$ are the same, within the experimental uncertainty. Conversely, we find $\Delta H^{\#}(D_2^{16}O) > \Delta H^{\#}(H_2^{16}O)$. Given that the reorientation of water molecules is associated with hydrogen-bond breaking,[39,58] $\Delta H^{\#}$ is intimately related to the hydrogen bond strength.[34] As such, the observation of $\Delta H^{\#}(D_2^{16}O) > \Delta H^{\#}(H_2^{16}O)$ is consistent with $D_2^{16}O$ forming stronger hydrogen bonds than $H_2^{16}O$.[5,59] Furthermore, the $\sim$12% higher activation entropy of $D_2^{16}O$ relative to $H_2^{16}O$ supports the notion that $D_2^{16}O$ is more structured than $H_2^{16}O$.[5,19,20,23,24] Overall, our results indicate that an increase in τ_c upon H/D substitution arises predominantly from the higher $\Delta H^{\#}(D_2^{16}O)$ relative to $\Delta H^{\#}(H_2^{16}O)$. Conversely, we detect no significant difference between the activation parameters of $H_2^{16}O$ and $H_2^{18}O$, indicating close structural similarity and similar interaction strengths of their hydrogen-bonding networks, in line with the findings of a previous X-ray diffraction study.[22]

Table 1 Fitted parameters for the enthalpy ($\Delta H_{ref}^{\#}$, $T = 298$ K), entropy ($\Delta S_{ref}^{\#}$, $T = 298$ K) and heat capacity ($\Delta c_p^{\#}$) of activation for the cooperative relaxation time of $H_2^{16}O$, $H_2^{18}O$ and $D_2^{16}O$, as obtained in the present work (p.w.) and in literature. Also shown is the standard error of each parameter

Species	$\Delta H_{ref}^{\#}$/kJ mol^{-1}	$\Delta S_{ref}^{\#}$/J mol^{-1} K^{-1}	$\Delta c_p^{\#}$/J mol^{-1} K^{-1}	Ref.
$H_2^{16}O$	16.1 ± 0.2	21.1 ± 0.7	-94 ± 12	p.w.
	15.9 ± 0.2	20.4 ± 0.7	-160 ± 22	39
	16.2	20.5	-138	57
$H_2^{18}O$	16.2 ± 0.3	21.2 ± 0.9	-103 ± 15	p.w.
$D_2^{16}O$	17.4 ± 0.3	23.6 ± 0.9	-115 ± 20	p.w.
	17.4	23.8	-138	57

5470 | *Phys. Chem. Chem. Phys.*, 2021, **23**, 5467–5473

This journal is © the Owner Societies 2021

The effect of viscosity on the relaxation dynamics

As the Stokes–Einstein–Debye equation[45] predicts τ_c to be proportional to the macroscopic viscosity η, we first investigate the relationship between τ_c and η. For both $H_2^{16}O$ and $D_2^{16}O$, our data for τ_c indeed scale linearly with η (viscosity data were taken from ref. 2), but this variation is not identical for the two isotopic species (see Fig. S3, ESI†). For $H_2^{18}O$, although literature data for its viscosity are scarce and limited to 288–308 K,[1] we find that the plots of τ_c vs. η for $H_2^{16}O$ and $H_2^{18}O$ collapse onto a single line (Fig. S3, ESI†), indicating that the relaxation times are affected by viscosity in the same manner.

To gain further information about the isotope effects, it is instructive to compare the enhancements of the viscosities and relaxation times. In Fig. 4a, we show the plots of $\tau_c(D_2^{16}O)/\tau_c(H_2^{16}O)$ vs. $\eta(D_2^{16}O)/\eta(H_2^{16}O)$ together with $\tau_c(H_2^{18}O)/\tau_c(H_2^{16}O)$ vs. $\eta(H_2^{18}O)/\eta(H_2^{16}O)$. In the case of $^{16}O/^{18}O$ substitution, we find that both τ_c and η increase by a factor of ~ 1.04–1.05, independent of temperature. As such, viscosity and relaxation times are equally affected by the replacement of oxygen with heavy oxygen. Hence, similar to viscosity,[1,5,8] the difference between $\tau_c(H_2^{18}O)$ and $\tau_c(H_2^{16}O)$ can be described by the square root of their masses:

$$\tau_c\left(H_2^{18}O, T\right) = \sqrt{\frac{M\left(H_2^{18}O\right)}{M(H_2^{16}O)}} \cdot \tau_c\left(H_2^{16}O, T\right) \qquad (6)$$

This is demonstrated in Fig. 4b, which shows that the values of $\tau_c(H_2^{18}O)$ divided by the translational mass factor fall onto the fitted curve of $\tau_c(H_2^{16}O)$. This proportionality suggests that the isotope enhancement of τ_c is governed by the same translational mass factor $\sqrt{M(H_2^{18}O)/M(H_2^{16}O)} \approx \sqrt{1.13} \approx 1.054$ as found for viscosity.[1,5,8] Rotational motions, which would scale with the square root of the ratio of the moments of inertia ($\approx \sqrt{1.006} \approx 1.003$), seem to play a minor role.

Fig. 4a shows that the relative increase in the relaxation time and viscosity upon H/D exchange is more pronounced (~ 15–35%) than for $^{16}O/^{18}O$ substitution (~ 4–5%), which therefore cannot be explained solely by translational mass effects. Rather, the temperature dependence of both ratios is a strongly indicative of nuclear quantum effects.[8] For viscosity, such differences between $D_2^{16}O$ and $H_2^{16}O$ have been accounted for by an apparent temperature shift ($\Delta T = 6.5$ K) in addition to the translational mass factor.[2–4] Based on the strong correlation between the ratios of $\tau_c(D_2^{16}O)/\tau_c(H_2^{16}O)$ and $\eta(D_2^{16}O)/\eta(H_2^{16}O)$, we test an analogous empirical relationship for $\tau_c(D_2^{16}O)$ and $\tau_c(H_2^{16}O)$:

$$\tau_c\left(D_2^{16}O, T\right) = \sqrt{\frac{M\left(D_2^{16}O\right)}{M(H_2^{16}O)}} \cdot \tau_c\left(H_2^{16}O, T - \Delta T\right) \qquad (7)$$

The data in Fig. 4b show that the values of $\tau_c(D_2^{16}O)$ show minimal deviations from the data for $\tau_c(H_2^{16}O)$ by taking the mass factor (1.054) into account and scaling the temperature for $D_2^{16}O$ by $\Delta T = 7.16$ K (see also Fig. S4 in the ESI†). We note that when we perform this fit by treating the mass factor ($\sqrt{M(D_2^{16}O)/M(H_2^{16}O)}$ in eqn (7)) as an adjustable parameter, we obtain this factor to be 1.054, in quantitative agreement with $\sqrt{M(D_2^{16}O)/M(H_2^{16}O)}$ (Fig. S5, ESI†). As such, our data strongly suggest that classical mass effects on the dielectric relaxation time scale with the square root of water's molecular mass.

The determined value for $\Delta T = 7.16$ K is in close agreement with $\Delta T = 7.2$ K obtained earlier from THz spectroscopic measurements (performed at $\nu > 100$ GHz),[16] although in ref. 16 the mass factor has not been included. Interestingly, the enhancement for τ_c upon H/D exchange is consistently higher than for η (Fig. 4a), in line with previous findings.[6,9,12] Given the mass factor is the same for both quantities, this difference is reflected by the higher ΔT for τ_c, as compared to the temperature shift reported for η ($\Delta T = 6.5$ K).[2–4] Hence, the slightly different isotope effect for viscosity and relaxation time upon H/D exchange suggests that the role of the relevant molecular motions involved in the thermal activation of viscous flow and dipolar reorientation are somewhat different.

Conclusions

We study the effect of isotopic substitution on the dielectric relaxation of water at temperatures ranging from 278 to 338 K. In line with earlier reports on $H_2^{16}O$, the spectra of $D_2^{16}O$ and $H_2^{18}O$ at frequencies ranging from 0.05 to 125 GHz can be excellently described with two Debye relaxations. The dominant relaxation is centered at 8–40 GHz – depending on temperature and isotopic composition – and has been ascribed to the cooperative dipolar rearrangement of water's three-dimensional hydrogen-bonded network. Upon H/D exchange, we find a 20–35% increase in the corresponding relaxation time, whereas $^{16}O/^{18}O$ substitution results in a markedly weaker (~ 4–5%) slow-down of the dynamics. Analysis of the thermal activation of the relaxation using the extended Eyring theory shows that the activation parameters for
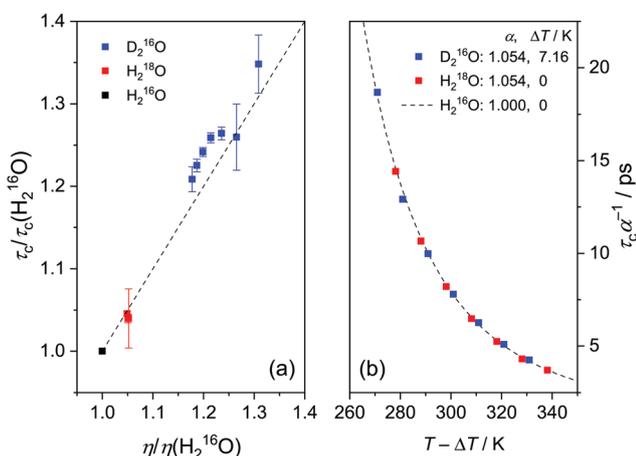

Fig. 4 (a) Enhancement of the relaxation time of the collective relaxation (τ_c) as a function of viscosity enhancement for $H_2^{16}O$, $H_2^{18}O$ as well as $D_2^{16}O$ relative to $H_2^{16}O$. Symbols represent experimental data together with the dashed line through the origin with unity slope. (b) Scaled τ_c for $H_2^{16}O$, $H_2^{18}O$, and $D_2^{16}O$ as a function of temperature. Symbols represent experimental data divided by the mass factor, $\alpha = (M(\text{isotope})/M(H_2^{16}O))^{1/2} = 1.054$ and shifted on the temperature scale by ΔT. The dashed line is the fitted curve of $\tau_c(H_2^{16}O)$, based on eqn (3)–(5) and the parameters listed in Table 1.

$H_2^{16}O$ and for $H_2^{18}O$ are virtually the same. For $D_2^{16}O$, the enthalpy of activation is higher than for $H_2^{16}O$, in line with stronger hydrogen-bonding of $D_2^{16}O$.

We find that the increase in the relaxation time of $H_2^{18}O$ relative to $H_2^{16}O$ is invariant of temperature suggesting that the isotope effect is dominated by (temperature independent) classical mass effects. The enhancement upon $^{16}O/^{18}O$ substitution can be well described by the translational mass factor $\sqrt{M(H_2^{18}O)/M(H_2^{16}O)}$, despite the dipolar relaxation of water having rotational character, for which one would expect the moments of inertia to determine the relaxation time. The increase in the relaxation time is in quantitative agreement with the increase in the viscosity, indicating that the slow-down of the relaxation dynamics of $H_2^{18}O$ is governed by higher viscous friction.

Conversely, upon H/D exchange, the increase in relaxation time is markedly higher and exhibits strong temperature dependence. Nevertheless, the relaxation times of $D_2^{16}O$ coincide with those of $H_2^{16}O$ when scaling with the translational mass factor and accounting for nuclear quantum effects with an apparent temperature shift. We find this temperature shift for the dielectric relaxation time to be larger (7.16 K) than that for viscosity (6.5 K [2–4]). Hence, despite the dielectric relaxation of water being intimately related to viscosity, the different temperature shifts point towards subtly different molecular motions involved in the thermal activation of the corresponding dynamics.

Conflicts of interest

There are not conflicts of interest to declare.

Acknowledgements

References

1 A. I. Kudish, D. Wolf and F. Steckel, *J. Chem. Soc., Faraday Trans.*, 1972, **68**, 2041–2046.

2 C. H. Cho, J. Urquidi, S. Singh and G. W. Robinson, *J. Phys. Chem. B*, 1999, **103**, 1991–1994.

3 K. L. Harris, *Phys. Chem. Chem. Phys.*, 2002, **4**, 5841–5845.

4 K. L. Harris and L. A. Woolf, *J. Chem. Eng. Data*, 2004, **49**, 1064–1069.

5 M. Ceriotti, W. Fang, P. G. Kusalik, R. H. McKenzie, A. Michaelides, M. A. Morales and T. E. Markland, *Chem. Rev.*, 2016, **116**, 7529–7550.

6 E. H. Hardy, A. Zygar, M. D. Zeidler, M. Holz and F. D. Sacher, *J. Chem. Phys.*, 2001, **114**, 3174–3181.

7 S. E. Lappi, B. Smith and S. Franzen, *Spectrochim. Acta, Part A*, 2004, **60**, 2611–2619.

8 A. Berger, G. Ciardi, D. Sidler, P. Hamm and A. Shalit, *Proc. Natl. Acad. Sci. U. S. A.*, 2019, **116**, 2458–2463.

9 C. H. Collie, J. B. Hasted and D. M. Ritson, *Proc. Phys. Soc., London*, 1948, **6**, 145–160.

10 P. S. Yastremskii, *J. Struct. Chem.*, 1971, **12**, 483–484.

11 A. A. Zharkikh, A. K. Lyashchenko, V. S. Kharkin, V. V. Goncharov and A. S. Lileev, *Russ. J. Phys. Chem.*, 1991, **65**, 553–557.

12 U. Kaatze, *Chem. Phys. Lett.*, 1993, **203**, 1–44.

13 C. Hölzl, PhD thesis, University of Regensburg, 1998.

14 K. Okada, M. Yao, Y. Hiejima, H. Kohno and Y. Kajihara, *J. Chem. Phys.*, 1999, **110**, 3026–3036.

15 S. Schrödle, PhD thesis, University of Regensburg, 2005.

16 C. Rønne and S. R. Keiding, *J. Mol. Liq.*, 2002, **101**, 199–218.

17 H. Yada, M. Nagai and K. Tanaka, *Chem. Phys. Lett.*, 2009, **464**, 166–170.

18 P. Zalden, L. Song, X. Wu, H. Huang, F. Ahr, O. D. Mücke, J. Reichert, M. Thorwart, P. K. Mishra, R. Welsch, R. Santra, F. X. Kärtner and C. Bressler, *Nat. Commun.*, 2018, **9**, 1–7.

19 S. A. Kuharski and P. J. Rossky, *J. Chem. Phys.*, 1985, **82**, 5164–5177.

20 J. S. Badyal, D. L. Price, M.-L. Saboungi, D. R. Haeffner and S. R. Shastri, *J. Chem. Phys.*, 2002, **116**, 10833–10837.

21 L. Hernández de la Peña and P. G. Kusalik, *J. Chem. Phys.*, 2004, **121**, 5992–6002.

22 R. T. Hart, C. J. Benmore, J. Neuefeind, S. Kohara, B. Tomberli and P. A. Egelstaff, *Phys. Rev. Lett.*, 2005, **94**, 047801.

23 U. Bergmann, D. Nordlund, P. Wernet, M. Odelius, L. G. M. Pettersson and A. Nilsson, *Phys. Rev. B: Condens. Matter Mater. Phys.*, 2007, **76**, 024202.

24 A. K. Soper and C. J. Benmore, *Phys. Rev. Lett.*, 2008, **108**, 065502.

25 T. Clark, J. Heske and T. D. Kühne, *ChemPhysChem*, 2019, **20**, 2461–2465.

26 F. Paesani, S. Iuchi and G. A. Voth, *J. Chem. Phys.*, 2007, **127**, 074506.

27 P. Hamm, G. S. Fanourgakis and S. S. A. Xantheas, *J. Chem. Phys.*, 2017, **147**, 064506.

28 F. Steckel and S. Szapiro, *Trans. Faraday Soc.*, 1963, **59**, 331–343.

29 K. R. Harris and L. A. Woolf, *J. Chem. Soc., Faraday Trans. 1*, 1980, **76**, 377–385.

30 S. Perticaroli, B. Mostofian, G. Ehlers, J. C. Neuefeind, S. O. Diallo, C. B. Stanley, L. Daemen, T. Egami, J. Katsaras, X. Cheng and J. D. Nickels, *Phys. Chem. Chem. Phys.*, 2017, **19**, 25859–25869.

31 T. Iwashita, B. Wu, W.-R. Chen, S. Tsutsui, A. Q. R. Baron and T. Egami, *Sci. Adv.*, 2017, **3**, e1603079.

32 T. Yamaguchi, *J. Phys. Chem. B*, 2018, **122**, 1255–1260.

5472 | *Phys. Chem. Chem. Phys.*, 2021, **23**, 5467–5473

This journal is © the Owner Societies 2021

33 A. Yahya, L. Tan, S. Perticaroli, E. Mamontov, D. Pajerowski, J. Neuefeind, G. Ehlers and J. D. Nickels, *Phys. Chem. Chem. Phys.*, 2020, **22**, 9494–9502.

34 H. Eyring, *J. Chem. Phys.*, 1936, **4**, 283–291.

35 J. Teixeira, M.-C. Bellissent-Funel, S. H. Chen and A. J. Dianoux, *Phys. Rev. A: At., Mol., Opt. Phys.*, 1985, **31**, 1913–1917.

36 D. Manogaran and Y. Subramanian, *J. Phys. Chem. B*, 2017, **121**, 11344–11355.

37 A. Shalit, S. Ahmed, S. Savolainen and P. Hamm, *Nat. Chem.*, 2017, **9**, 273–278.

38 N. Agmon, *J. Phys. Chem.*, 1996, **100**, 1072–1080.

39 R. Buchner, J. Barthel and J. Stauber, *Chem. Phys. Lett.*, 1999, **306**, 57–63.

40 I. Popov, P. B. Ishai, A. Khamzin and Y. Feldman, *Phys. Chem. Chem. Phys.*, 2016, **18**, 13941–13953.

41 D. C. Elton, *Phys. Chem. Chem. Phys.*, 2017, **19**, 18739–18749.

42 U. Kaatze, *J. Mol. Liq.*, 2018, **259**, 304–318.

43 M. Sharma, R. Resta and R. Car, *Phys. Rev. Lett.*, 2007, **98**, 247401.

44 E. H. Grant, *J. Chem. Phys.*, 1957, **26**, 1575–1577.

45 C. Rønne, L. Thrane, P.-O. Åstrand, A. Wallqvist, K. V. Mikkelsen and S. R. Keiding, *J. Chem. Phys.*, 1997, **107**, 5319–5331.

46 P. Kumar, *Proc. Natl. Acad. Sci. U. S. A.*, 2006, **103**, 12955–12956.

47 J. W. C. Johns, *J. Opt. Soc. Am. B*, 1985, **2**, 1340–1354.

48 F. Kremer and A. Schönhals, in *Broadband Dielectric Spectroscopy*, ed. F. Kremer and A. Schönhals, Springer, Berlin-Heidelberg, 2003, ch. 1, pp. 1–33.

49 J. T. Kindt and C. A. Schuttenmaer, *J. Phys. Chem.*, 1996, **100**, 10373–10379.

50 T. Fukasawa, T. Sato, J. Watanabe, Y. Hama, W. Kunz and R. Buchner, *Phys. Rev. Lett.*, 2005, **95**, 197802.

51 A. Y. Zasetsky, *Phys. Rev. Lett.*, 2011, **107**, 117601.

52 N. Q. Vinh, M. S. Sherwin, S. J. Allen, D. K. George, A. J. Rahmani and K. W. Plaxco, *J. Chem. Phys.*, 2015, **152**, 164502.

53 V. Balos, S. Imoto, R. R. Netz, M. Bonn, D. J. Bonthuis, Y. Nagata and J. Hunger, *Nat. Commun.*, 2020, **11**, 1611.

54 J. G. Kirkwood, *J. Chem. Phys.*, 1939, **7**, 911–919.

55 H. Fröhlich, *Theory of Dielectrics*, Clarendon Press, Oxford, 1958.

56 S. Glasstone, K. J. Laidler and H. Eyring, *The Theory of Rate Processes*, McGraw-Hill, New York, 1941.

57 B. E. Conway, *Can. J. Chem.*, 1959, **37**, 613–628.

58 D. Laage and J. T. Hynes, *Science*, 2006, **311**, 832–835.

59 Q. Hu, S. Ouyang, J. Li and Z. Cao, *J. Raman Spectrosc.*, 2017, **48**, 610–617.

This journal is © the Owner Societies 2021

Phys. Chem. Chem. Phys., 2021, **23**, 5467–5473 | **5473**